Title

Histologic and immunohistochemical predictors of clinical behavior for feline diffuse iris melanoma

Authors

Wiggans, K Tomo
Reilly, Christopher M
Kass, Philip H
et al.

Publication Date

2016-07-01

DOI

10.1111/vop.12344

Peer reviewed

Veterinary Ophthalmology (2016) 1–12 DOI:10.1111/vop.12344

Histologic and immunohistochemical predictors of clinical behavior for feline diffuse iris melanoma

K. Tomo Wiggans,*[,1] Christopher M. Reilly,† Philip H. Kass‡ and David J. Maggs§

**William R. Pritchard Veterinary Medical Teaching Hospital, University of California, Davis, CA 95616, USA; †Departments of Pathology, Microbiology, and Immunology, University of California, Davis, CA 95616, USA; ‡Population Health and Reproduction, University of California, Davis, CA 95616, USA; and §Surgical and Radiological Sciences, University of California, Davis, CA 95616, USA*

Address communications to:

David J. Maggs

Tel.: (530) 752-1393
Fax: (530) 752-6042
e-mail: djmaggs@ucdavis.edu

[1]Present address: Bay Area Animal Eye Care, 2100 Monument Boulevard, Suite 7, Pleasant Hill, CA 94523, USA

Abstract

Objective To determine histologic and immunohistochemical predictors of metastasis of feline diffuse iris melanoma (FDIM).

Animals Globes from 47 client-owned cats enucleated for FDIM between January 1985 and December 2013.

Procedures Hematoxylin and eosin-stained sections were evaluated for neoplastic invasiveness and cell morphology, necrosis within the neoplasm, inflammation, and glaucoma. Sections were immunolabeled with antibodies against melan-A, PNL2, E-cadherin, or B-Raf, and label intensity, percentage of labeled cells, and label homogeneity were semi-quantitatively graded. Medical records were evaluated, and referring veterinarians and clients were contacted to determine whether cats developed metastasis following enucleation. The log-rank test or Cox proportional hazards model was used to determine associations between histologic or immunohistochemical parameters and metastasis.

Results Metastasis was suspected or confirmed in 9/47 (19%) cats. Extrascleral extension, necrosis within the neoplasm, a mitotic index of >7 mitoses in 10 high-power (×400) fields, choroidal invasion, and increased E-cadherin and melan-A label intensity were each associated with increased rate of metastasis. PNL2 label homogeneity was associated with decreased rate of metastasis. Decreased PNL2 label intensity and an increasing percentage of neoplastic cells labeled for melan-A each approached significance for increased rate of metastasis.

Conclusions We report four histologic and three immunohistochemical parameters helpful in determining cats at risk of metastasis of FDIM. Further studies should determine if B-Raf mutations identified in human malignant melanomas are found in cats with FDIM and assess benefits of adjunctive therapy following enucleation of eyes with FDIM bearing poor prognostic indicators.

Key Words: B-Raf, E-cadherin, feline diffuse iris melanoma, melan-A, pheomelanin, PNL2

INTRODUCTION

The eye is the most common location for feline melanocytic neoplasia[1,2] with feline diffuse iris melanoma (FDIM) accounting for 26% of feline submissions to, and 50% of feline neoplasms diagnosed by, an ocular pathology laboratory.[3] Feline diffuse iris melanomas typically begin as flat, hyperpigmented foci on the iris, but progress to affect larger portions of the iris, ciliary body, iridocorneal angle, and sclera, often in association with uveitis or glaucoma.[4,5] Metastatic rates of 24–63% have been reported[1,4] with metastasis typically occurring to distant organs, including liver, lung, spleen, lymph nodes, and bone.[1,4,6] Adjunctive therapy protocols following enucleation of globes with FDIM are not established. Additionally, progression and metastasis of FDIM are unpredictable with some early neoplasms metastasizing more rapidly,[1] and many locally advanced neoplasms not metastasizing. The only clinical

prognostic indicator described for FDIM is the presence of secondary glaucoma, which carries a worsened prognosis.[5] In addition to being a poor prognostic indicator, the presence of secondary glaucoma in eyes affected by FDIM often warrants enucleation due to associated discomfort. By contrast, multiple histologic features associated with survival have been identified, but only following enucleation. Specifically, increased mitotic index[4] and neoplastic invasion of the ciliary body,[5] sclera,[5] and/or scleral venous plexus[4,5] have each been associated with decreased survival. Because of the relative lack of clinical prognostic indicators, close monitoring and early removal of globes affected with pigmentary changes characteristic of FDIM are sometimes recommended.[5,7]

Due to the lack of clinical and histologic prognostic indicators, this study was designed to assess four molecular markers of potential value in prognostication for FDIM: melan-A, PNL2, E-cadherin, and B-Raf. Melan-A is an antigen expressed by cells of melanocyte origin. *In vitro* studies of cell lines obtained from canine cutaneous melanocytic neoplasms have shown decreased expression of melan-A in malignant neoplasms relative to benign neoplasms.[8] Additionally, silencing of the melan-A gene (*MART1*) in a human uveal malignant melanoma cell line which expressed melan-A was associated with increased migration of cultured cells and down-regulation of expression of a metastasis suppressor gene, *NM23*, compared to control cell lines.[9] Finally, human patients with cutaneous malignant melanomas that expressed melan-A had longer survival times than those who did not.[10] PNL2 is an antibody directed against an unidentified antigen also expressed by normal and neoplastic melanocytes,[11] but whose prognostic value in human and feline melanocytic neoplasms is unknown. E-cadherin is a transmembrane protein responsible for cell adhesion. Down-regulation of E-cadherin is associated with metastasis in a range of neoplasms, including human cutaneous malignant melanomas.[12] B-Raf is a proto-oncogene product with a role in the mitogen-activated protein kinase (MAPK) signaling pathway.[13–16] Gain-of-function mutations in B-Raf have been identified in human cutaneous and uveal malignant melanomas[14,17,18] and are of particular importance because inhibitors of B-Raf and other kinases are currently being investigated as adjunctive chemotherapeutic agents.[19–22] Despite the increasing appreciation of the value of these markers in other neoplasms or uveal melanocytic neoplasms of other species, to the authors' knowledge, studies investigating the prognostic value in FDIMs of melanocyte antigens, cellular adhesion molecules, and oncogenes/proto-oncogenes are lacking. Meanwhile, improved understanding of the biological behavior of FDIM at the molecular level would be of extraordinary clinical value. Validated molecular diagnostic assays could be used to guide decision-making regarding staging and therapy, especially if they could be used on cytologic samples gained by intraocular aspiration or incisional uveal biopsies rather than enucleated globes, as this would permit clinicians to preserve what are typically visual and comfortable eyes. Additionally, given the increasing specificity of some chemotherapeutic agents, identification of target molecules could help clinicians to design individualized antineoplastic therapy in multiple species.

We hypothesized that FDIMs in globes enucleated from cats that developed metastasis would be more likely to display increased histologic indicators of aggressiveness (including extension beyond the iris, inflammation, and/or glaucoma); decreased expression of melan-A, PNL2, and E-cadherin; and increased expression of B-Raf relative to FDIMs which had not been demonstrated to metastasize. Ultimately, we believe that a panel of validated immunohistochemical markers will be useful to determine which patients may benefit from adjunctive treatment following surgery, and may help to identify effective, targeted therapies. Therefore, the purpose of this study was to evaluate FDIM-affected, enucleated globes from a population of cats in which follow-up information regarding metastasis was available, so as to determine histologic and immunohistochemical predictors of metastasis.

MATERIALS AND METHODS

Sample population

The University of California (UC), Davis, Veterinary Medical Teaching Hospital (VMTH) pathology database was searched for all globes diagnosed with FDIM between January 1, 1985 and December 31, 2013. Cases diagnosed with, or subsequently interpreted as, iridal melanosis were excluded. This collection includes globes from cats enucleated by members of the Ophthalmology Service at the UC Davis VMTH as well as external submissions to the UC Davis Comparative Ocular Pathology Service. Medical records for affected cats were reviewed for data regarding breed, sex, age, affected eye, and a clinical diagnosis of glaucoma; dates of initial presentation and enucleation; histopathologic diagnosis; and staging, especially necropsy data and diagnostic test results. For patients presented to the UC Davis VMTH for enucleation, data were obtained directly from the electronic medical record. For patients from which eyes were submitted by external practitioners, all referring veterinarians were contacted by telephone or email. For cats in which follow-up information was not available in this manner, owners were contacted by phone or email. All data retrieval was carried out in a consistent manner by a single author (KTW). For the purposes of this study, metastasis was defined as 'confirmed' if melanocytic neoplasia at a nonocular site was diagnosed using cytology and/or histopathology, or as 'suspected' if there was radiographic or ultrasonographic evidence consistent with metastatic disease.

Histopathologic evaluation

Archived, hematoxylin and eosin-stained parasagittal sections of enucleated globes were evaluated; sections were recut and restained if stain quality was considered poor. Specimens submitted prior to 2004 were fixed in Bouin's solution for 12–24 h and rinsed in 70% ethanol. Subsequent specimens were fixed in 10% neutral-buffered formalin for 12–24 h for internal submissions and up to 96 h for external submissions that required shipping. Because fixative choice can affect immunohistochemistry (IHC) results, quality of immunohistochemical labeling of samples fixed in Bouin's solution was compared to positive controls, and formalin-fixed specimens; if poor labeling secondary to fixative type was noted, all samples fixed in that way were excluded from analysis. Sections were evaluated for the extent of invasion of atypical melanocytes (i.e., cells with at least some morphologic features of atypia such as increased nuclear to cytoplasmic ratio, nucleoli, and/or mitotic figures). The presence of neoplastic melanocytes on the anterior iris surface was recorded, and the degree of invasion was defined anatomically as involving the iris stroma, trabecular meshwork, ciliary body, choroid, or sclera. Disruption of the iris pigment epithelium, extrascleral extension, or scleral vascular invasion by neoplastic cells was also recorded. Neoplasms were evaluated for the presence of necrosis. Overall neoplastic cell morphology was classified as epithelioid, spindle, or mixed, and presence or absence of neoplastic cells with 'balloon cell' morphology (cells with abundant pale to clear or vacuolated cytoplasm with variable melanin density) was recorded. Neoplastic cells were semi-quantitatively graded for anisocytosis, anisokaryosis, and degree of pigment intensity (none, mild, moderate, marked), and percentage of neoplastic cells containing melanin (0%, 1–25%, 26–50%, 51–75%, 76–100%). Mitotic index was defined as number of mitotic figures noted in 10 high-power (×400) fields (HPF). Globes were evaluated for uveal inflammation and glaucoma (present or absent). Two investigators (CMR, KTW) jointly reviewed all sections and came to a consensus on all assessments.

Immunohistochemical optimization for B-Raf

The putative feline B-Raf amino acid sequence was obtained from an online source (www.ensembl.org). Assessment with an online basic local alignment search tool (BLAST; blast.ncbi.nlm.nih.gov) revealed 93% sequence homology with the human wild-type B-Raf. Two anti-B-Raf antibodies (polyclonal rabbit anti-human, Abnova #18511 and #3946, Taipei City, Taiwan) were selected because the proprietary target epitopes were 100% homologous with the corresponding region within the putative feline B-Raf amino acid sequence. Tissues used as positive and negative controls were based on manufacturer recommendations for human tissue as well as immunohistochemical labeling of normal human tissues identified in the Human Protein Atlas (www.proteinatlas.org), namely normal canine and feline testis and feline rectum for positive controls, and normal feline colon and lung as negative controls. Slides were deparaffinized and rehydrated in xylene and graded alcohols, prior to 10 min blocking against endogenous peroxidases using 0.03% hydrogen peroxide in 4% methanol (Dako, Carpinteria, CA, USA). Slides were then rinsed three times with phosphate-buffered saline (PBS; pH 7.4) + 0.5% Tween before 1 set of slides was subjected to heat antigen retrieval using a microwave, while a duplicate set of slides was not subjected to any form of antigen retrieval. Tissues were blocked with 10% heat-inactivated equine serum in PBS for 20 min at 22 °C. Doubling dilutions of anti-B-Raf antibody from 1:100 to 1:400 were applied to slides for 30 min at 22 °C in a humidified chamber. Slides were again rinsed three times with PBS + 0.5% Tween. Three to five drops of biotinylated goat anti-rabbit IgG (Biocare 4+ goat anti-rabbit IgG, #GR608; Biocare Medical, Concord, CA, USA) were applied and incubated for 13 min at 22 °C in a humidified chamber. Slides were again rinsed three times with PBS + 0.5% Tween. Three to five drops of streptavidin horseradish peroxidase label (Biocare 4+ horseradish peroxidase, #HP604; Biocare Medical) were applied and incubated for 10 min at 22 °C in a humidified chamber. Slides were again rinsed three times with PBS + 0.5% Tween. Horseradish peroxidase substrate (NovaRed, Vector Labs, Burlingame, CA, USA) was prepared according to the manufacturer's instructions, and 3–5 drops were applied to slides for approximately 30 s at 22 °C. Slides were rinsed in deionized water for 5 min. Mayer's hematoxylin was applied to slides for 6 s at 22 °C, and slides were subsequently washed in tap water until all counterstain was removed. Slides were air-dried overnight, and a coverslip was placed with the aid of Shandon-Mount mounting medium (ThermoFisher Scientific, Waltham, MA, USA). Abnova anti-B-Raf antibody #18511 at a dilution of 1:100 and without heat antigen retrieval provided the strongest and most consistent labeling of positive samples; however, a 1:200 dilution also provided adequate results while requiring less antibody per sample. Once optimized, the protocol was used to batch process all ocular specimens.

Immunohistochemical evaluation

Archived paraffin-embedded enucleated globes were serially sectioned at 5 μm for all IHC. In addition to the FDIM samples, a histologically normal formalin-fixed globe from a cat euthanized for reasons unrelated to this study was also sectioned to evaluate the labeling characteristics of normal iris melanocytes. Immunohistochemistry for melan-A, PNL2, and E-cadherin was performed routinely using protocols currently in place in the UC Davis VMTH Histology Laboratory for veterinary diagnostic use. Briefly, all slides were deparaffinized in xylene and

rehydrated in graded alcohols, prior to 20 min blocking against endogenous peroxidases using 0.03% hydrogen peroxide in 4% methanol (Dako). Slides to be treated with anti-melan-A (monoclonal mouse anti-human, Vector Labs, #VP-M646) or anti-E-cadherin (BD Biosciences, San Jose, CA, USA) antibodies underwent heat antigen retrieval in citrate buffer (Dako ×10 citrate buffer, #S1699) at 100 °C for 30 min. Slides treated with anti-PNL2 (monoclonal mouse anti-human, Dako #N160187-2) or anti-B-Raf (polyclonal rabbit anti-human, Abnova #18511, Taipei City, Taiwan) antibodies did not require antigen retrieval. Antibody dilutions and incubation conditions for primary antibodies were as follows: melan-A, 1:200 for 3 h at 22 °C; PNL2, 1:100 for 30 min at 22 °C; E-cadherin, 1:500 for 30 min at 22 °C; B-Raf, 1:200 for 30 min at 22 °C. Phosphate-buffered saline was used as a negative control. Feline uveal melanocytes were used as an internal positive control for melanocyte markers. Bulbar conjunctival epithelium was used as an internal positive control for E-cadherin. Feline testis and rectal epithelium were used as positive controls for B-Raf. Following rinsing three times in PBS + 0.5% Tween, slides were incubated with biotinylated goat anti-rabbit secondary antibody (Biocare 4+ goat anti-rabbit IgG, #GR608; Biocare Medical) for 13 min at 22 °C and rinsed three times in PBS + 0.5% Tween. Slides were then incubated with streptavidin-conjugated horseradish peroxidase (Biocare 4+ horseradish peroxidase, #HP604; Biocare Medical) for 10 min at 22 °C and rinsed three times in PBS + 0.5% Tween. NovaRed chromagen detection system (Vector Labs) was reconstituted as per the manufacturer's instructions and used for development with standardized development times for each antibody, as determined by optimal chromagen intensity before the development of background. Chromagen development time was as follows: 9 min for melan-A, 5 min for PNL2, 8 min for E-cadherin, and 45 s for B-Raf. Slides were rinsed in deionized water for 5 min followed by placement of 3–5 drops of Mayer's hematoxylin counterstain for 6 s at 22 °C. Slides were rinsed in tap water and air-dried. Glass coverslips were applied with Shandon-Mount medium (ThermoFisher Scientific) and allowed to dry overnight. Following labeling, all sections were semi-quantitatively graded for percentage of positively labeled neoplastic cells (0%, 1–25%, 26–50%, 51–75%, 76–100%). Overall label intensity (i.e., the label intensity of ≥50% of neoplastic cells) was assessed semi-quantitatively (none, mild, moderate, strong) using an internally derived scale between the negative control (none) and the most intensely labeled slide (strong). Homogeneity of labeling across the neoplasm was noted as a binary variable (homogeneous or heterogeneous) based on the necrosis-independent variability noted at ×100 or lower magnification. Two investigators (CMR, KTW) jointly reviewed all sections and came to a consensus on all IHC assessments.

Statistical analysis

A log-rank test was used to determine which binary clinical, histopathological, and immunohistochemical parameters evaluated were significantly associated with the development of metastasis. For categorical variables, a Cox proportional hazards model was used. For each comparison, a P-value ≤0.05 was considered significant. Where possible, Kaplan–Meier plots of the estimates of metastasis-free probability vs. time were created for parameters in which statistical significance was demonstrated.

RESULTS

Sample population

Forty-seven globes (24 right eyes and 23 left eyes) from 47 cats diagnosed with FDIM and for which follow-up information was available were identified. The majority were domestic cats (30 short-haired, four medium-haired, seven long-haired), along with two Persians, and one each of Siamese, Burmese, Manx, and an unspecified breed. There were 23 male-castrated and 23 female-spayed cats, with one cat of unidentified sex and neuter status. Secondary glaucoma was diagnosed in 32 (68%) eyes and was not significantly associated with metastasis (P = 0.36). Median (range) time from initial presentation to enucleation was 20 days (0 days–10 years), and median (range) age at histopathologic diagnosis was 10.4 (2.8–23.1) years. Metastasis was suspected in seven cats based on thoracic radiographs (n = 1) or abdominal ultrasound (n = 6), or confirmed in two cats based upon necropsy with histopathology, for a total (confirmed or suspected) metastatic rate of 9/47 (19%) cats. Median (range) times from histopathologic diagnosis to the detection of metastasis [9.8 months (28 days–1.8 years)] or euthanasia due to suspected/confirmed metastasis [9.8 months (28 days–1.9 years)] were very similar.

Histopathologic evaluation

A histologic diagnosis of FDIM was confirmed in all cases (n = 47). Thirty-one neoplasms (66%) possessed a mixed epithelioid-spindle cell morphology, 16 (34%) were composed only of epithelioid cells, and none was composed solely of spindle cells. Balloon cells were detected in 12 (26%) of neoplasms. Neither cell morphology nor presence of balloon cells were associated with metastasis (P = 0.7–0.9). Median (range) mitotic index was 4 (0–100) mitoses in 10 HPF. Neoplastic cells were detected within the anterior iris and iris stroma of all cats and disrupted the posterior iris pigment epithelium in >75% of cats. Frequencies at which other histopathologic parameters were detected ranged widely (Table 1). Likewise, semi-quantitative assessment of neoplastic cell anisocytosis, anisokaryosis, and degree of pigment intensity, as well as percentage of neoplastic cells containing melanin also ranged widely (Table 2). Considering all histopathologic parame-

Table 1. Detection frequency for select histopathologic parameters in 47 globes with feline diffuse iris melanoma

Histopathologic parameter	Number of reports (%)
Neoplastic cells within	
Anterior iris	47 (100)
Iris stroma	47 (100)
Trabecular meshwork	46 (96)
Ciliary body	43 (91)
Sclera	30 (64)
Choroid	13 (28)
Iris pigment epithelium disruption	36 (77)
Uveal inflammation	30 (64)
Glaucoma	29 (62)
Scleral vascular invasion	26 (55)
Mitotic index >7	15 (32)
Necrosis within the neoplasm	15 (32)
Balloon cells	12 (26)
Extrascleral extension	9 (19)

Table 2. Detection frequency for select semi-quantitatively assessed histopathologic parameters in 47 globes with feline diffuse iris melanoma

Histologic parameter	Number of reports (%)
Percentage of neoplastic cells containing melanin	
0%	1 (2)
1–25%	9 (19)
26–50%	7 (15)
51–75%	7 (15)
76–100%	23 (49)
Neoplasm pigment intensity	
None	1 (2)
Mild	20 (43)
Moderate	16 (34)
Marked	10 (21)
Anisocytosis	
None	0 (0)
Mild	12 (26)
Moderate	28 (60)
Marked	7 (15)
Anisokaryosis	
None	0 (0)
Mild	22 (47)
Moderate	19 (40)
Marked	6 (13)

ters, four were significantly associated with increased rate of metastasis: extrascleral extension of neoplastic cells ($P = 0.039$), necrosis within the neoplasm ($P = 0.026$), >7 mitoses in 10 HPF ($P = 0.024$), and choroidal invasion ($P = 0.045$) (Fig. 1). Plots showing estimates of the probability of cats remaining metastasis-free as a function of time following a histologic diagnosis of FDIM with or without each of these four histopathologic parameters are shown in Fig. 2.

Immunohistochemical evaluation

Melan-A IHC results for Bouin's-fixed specimens ($n = 6$; 2 with confirmed/suspected metastasis) were excluded due to suboptimal labeling of internal control tissues (melanocytes, tapetal iridocytes). Other antibodies were not affected by fixation method. Thus, melan-A data were derived from 41 globes (7 with confirmed/suspected metastases) and PNL2, E-cadherin, and B-Raf data were derived from 47 globes (9 with confirmed/suspected metastases). Melan-A, PNL2, and E-cadherin were expressed by iridal melanocytes in the normal control cat and in all iridal regions unaffected by neoplasia in the study cats. By contrast, B-Raf was not expressed by normal iridal melanocytes (Fig. 3). The percentage of immunohistochemically labeled neoplastic cells ranged greatly for all four markers; however PNL2 labeling was detected in all globes and was present in the greatest percentage of cells compared with the other three markers assessed (Fig. 4). Likewise, label intensity ranged widely but was commonly mild or moderate for melan-A, E-cadherin, and B-Raf, and strong for PNL2 (Fig. 4). Representative photomicrographs of mild, moderate, and strong labeling of neoplastic melanocytes are shown in Fig. 5. The association between rate of metastasis and percentage of neoplastic cells that were labeled approached significance for melan-A (hazard ratio [HR] = 1.8; 95% confidence interval [CI] = 0.97–3.2; $P = 0.062$). There was no significant association between rate of metastasis and percentage of neoplastic cells that were labeled for PNL2 (HR = 2.1, 95% CI = 0.35–13.4, $P = 0.41$), E-cadherin (HR = 1.7, 95% CI = 0.8–3.5, $P = 0.17$), or B-Raf (HR = 1.5; 95% CI = 0.86–2.8; $P = 0.14$). There was a positive association between increased rate of metastasis and label intensity for melan-A (HR = 2.8; 95% CI = 1.2–6.9; $P = 0.023$) and E-cadherin (HR = 5.1; 95% CI = 1.1–23.8; $P = 0.036$) (Figs 3 and 4); this association approached significance for PNL2 (HR = 0.29; 95% CI = 0.076–1.1; $P = 0.072$), but significance was not detected for B-Raf (HR = 1.5; 95% CI = 0.66–3.7; $P = 0.31$). Homogenous IHC labeling was identified in 16 (39%), 24 (51%), 9 (20%), and 26 (55%) of globes labeled with melan-A, PNL2, E-cadherin, and B-raf, respectively. Homogenous labeling of PNL2 (Fig. 3) was associated with a decreased rate of metastasis ($P = 0.0082$), but no similar associations were detected for melan-A ($P = 0.42$), E-cadherin ($P = 0.30$), or B-Raf ($P = 0.30$). A plot showing an estimate of the probability of cats remaining metastasis-free as a function of time following a histologic diagnosis of FDIM with or without homogenous labeling of PNL2 is shown in Fig. 6.

DISCUSSION

The present study introduces three novel and further defines a fourth clinically useful histologic indicators of metastasis for cats with FDIM—specifically, extrascleral neoplastic extension, necrosis within the neoplasm, a mitotic index >7, and choroidal invasion. Although extrascleral extension, necrosis within the neoplasm, and choroidal

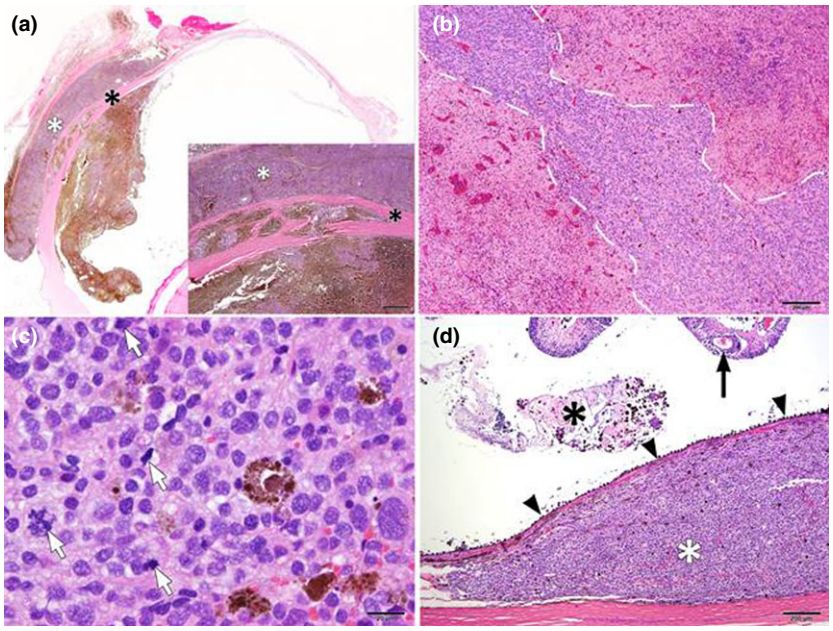

Figure 1. Representative examples of histologic features significantly associated with metastasis in globes with feline diffuse iris melanoma (FDIM) (hematoxylin and eosin). (a) Subgross image showing extension of neoplastic uveal cells (white asterisk) external to the sclera (black asterisk). Inset shows a higher magnification of the tumor (×20 magnification, bar = 500 μm). (b) A central band of viable neoplastic cells flanked by two regions of coagulative necrosis (dashed lines). Note the free pigment and absence of cellular architecture (×40 magnification, bar = 200 μm). (c) High mitotic index with four mitotic figures (arrowheads) evident in this single ×400 photomicrograph (a total of 40 mitoses in 10 HPF was seen for this case, all mitoses not shown) (×400 magnification, bar = 20 μm). (d) Choroidal invasion by neoplastic cells (white asterisk). A section of detached retina (arrow) and subretinal cellular and proteinaceous exudate (black asterisk) are also present in this image (×40 magnification, bar = 200 μm). Note hypertrophied retinal pigment epithelium overlying the neoplasm (arrowheads).

invasion have not previously been identified as risk factors for metastasis in cats with FDIM,[4,5] the association seems logical because they are typically indicators of rapid or infiltrative growth. Two studies of melanocytic neoplasia in dogs have shown that necrosis within the neoplasm is associated with a malignant phenotype; however, neither study investigated the association between necrosis and metastatic risk.[23,24] Furthermore, extraocular extension was detected more commonly in human uveal melanomas with necrosis than in those without necrosis.[25] We also confirmed and further defined the risk associated with a high mitotic index. Although this feature was previously associated with a worse prognosis, a specific cut-off value was not identified.[4] Our finding that a mitotic index >7 was associated with increased rate of metastasis may be of some immediate prognostic value for clinicians and pathologists, but requires further investigation and validation. It would be extremely useful to further assess this via quantification of a proliferation marker. For example, Ki67 is a prognostic indicator in canine melanocytic neoplasms,[26–29] with one report[26] also including feline melanocytic neoplasms of nonocular origin. Therefore, MIB1, the antibody against Ki67, should be applied to biopsy or cytology specimens from feline globes with benign nevi or FDIM as an association between mitotic index and MIB1 labeling, as well as associations between MIB1 labeling and risk of metastasis would be particularly useful.

Unlike previous studies which identified scleral venous plexus invasion by neoplastic cells as a negative prognostic indicator,[4,5] the present study failed to identify a similar association. Because only one section of each globe was assessed histologically in the present study, it is possible that invasion of the scleral vessels by neoplastic cells may have been missed; however, evaluation of only one section is routine in histologic practice. By contrast, we did identify a significant association between metastasis and both extrascleral extension and choroidal invasion of neoplastic cells in the present study. Therefore, it is possible that cats in the present study may have developed metastasis through invasion of blood vessels other than the scleral venous plexus. Neither a clinical diagnosis of glaucoma nor histologic evidence of glaucoma was associated with the development of metastasis in the present study. This is in contrast to a previous study which identified secondary glaucoma as a negative clinical prognostic indicator.[5] While it is still recommended that eyes with FDIM and uncontrolled secondary glaucoma be removed to restore comfort, the results of the present study suggest that these tumors can metastasize without first affecting the drainage of aqueous humor. Conversely, based on our data, the presence of glaucoma does not appear to increase metastasis rate, highlighting the difficulty of clinical prognostication and decision-making regarding the appropriate time to enucleate.

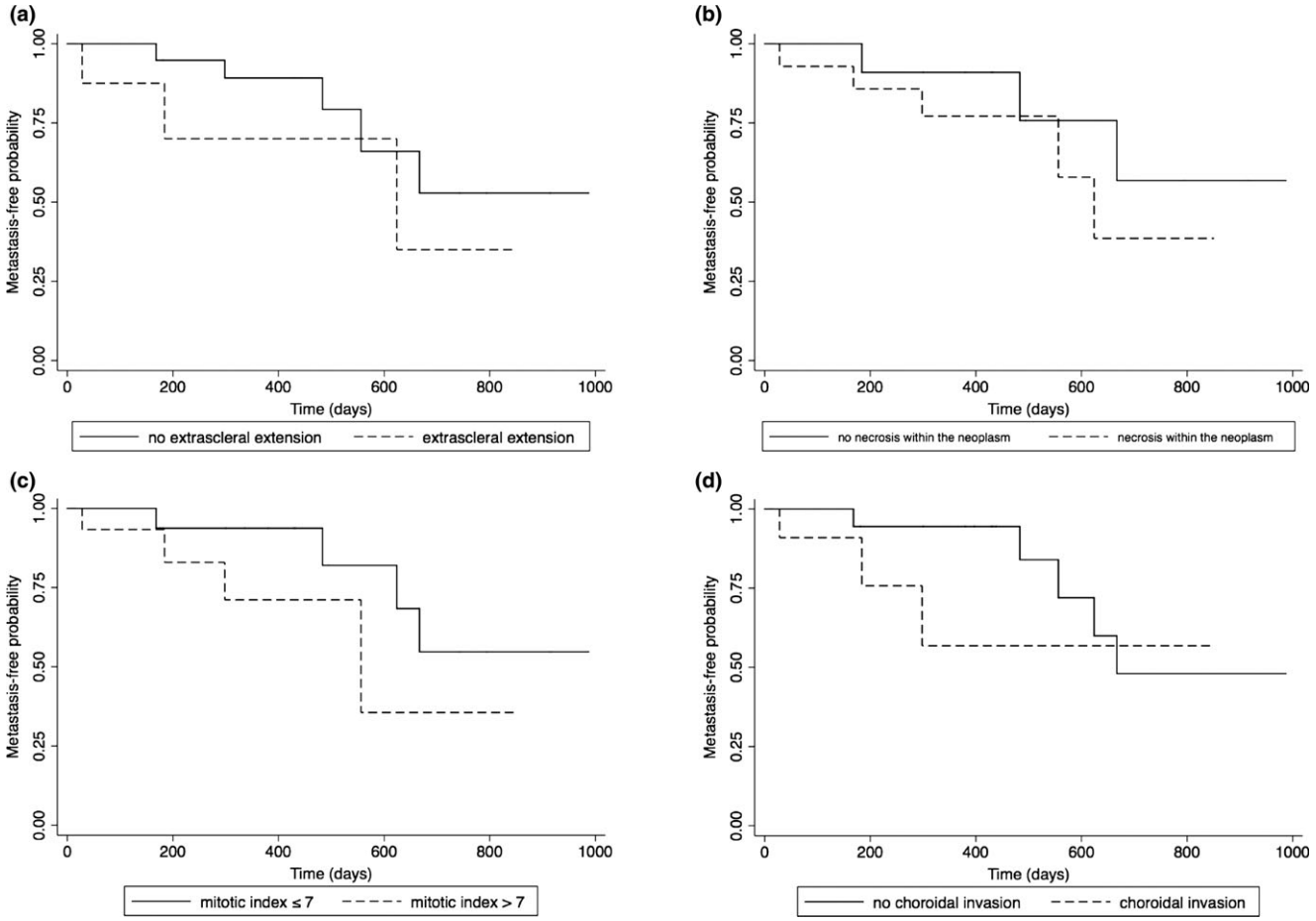

Figure 2. Kaplan–Meier plots showing the estimated probability of a cat remaining metastasis-free as a function of time following enucleation and histologic diagnosis of FDIM with or without (a) extrascleral extension of the neoplasm, (b) necrosis within the neoplasm, (c) a mitotic index >7, or (d) choroidal invasion.

Although immunohistochemical features of feline intraocular neoplasms have been described,[30] it has been performed only to assess association between neoplasms and lens capsule rupture or to aid in the diagnosis of poorly differentiated neoplasms. To the authors' knowledge, the present study is the first to identify immunohistochemical predictors of metastasis in FDIM. Here, we showed that increased label intensity of melan-A and E-cadherin was associated with an increased rate of metastasis and that homogenous labeling of PNL2 was associated with a decreased rate of metastasis. Furthermore, increased percentage of neoplastic cells labeled for melan-A and decreased PNL2 label intensity approached significance for increased rate of metastasis. Each of these markers warrants further discussion.

Melan-A (also known as MART-1) is the product of the *MLANA* gene and is considered less sensitive but more specific for the diagnosis of melanocytic neoplasms than are other immunohistochemical markers such as such as S100, vimentin, and neuron-specific enolase.[31,32] Our finding that increased melan-A label intensity was associated with metastatic potential of FDIM was in contrast to our hypothesis and suggests that neoplastic feline uveal melanocytes behave less like neoplastic cells within human and canine cutaneous melanocytic neoplasms. *In vitro* studies using cell cultures derived from canine oral or cutaneous melanocytic neoplasms revealed that cells from malignant neoplasms labeled weakly or not at all for melan-A, whereas those from benign neoplasms demonstrated moderate to strong labeling.[8] Similarly, human patients with positive expression of melan-A within cutaneous malignant melanoma cells survived longer than did those whose tumors were melan-A negative.[10] A histologic and immunohistochemical study of malignant melanomas of the head and neck in humans, however, failed to find any association between melan-A labeling and overall or metastasis-free survival.[33] The expression of melan-A as a prognostic indicator may be less clear. An *in vitro* study of human uveal malignant melanomas showed that silencing of the *MART-1* gene led to increased migration of cultured cells.[9] But an immunohistochemical study of human uveal malignant melanomas and metastatic lesions showed that all primary uveal and metastatic samples labeled for melan-A, whereas 17% of cutaneous malignant melanomas

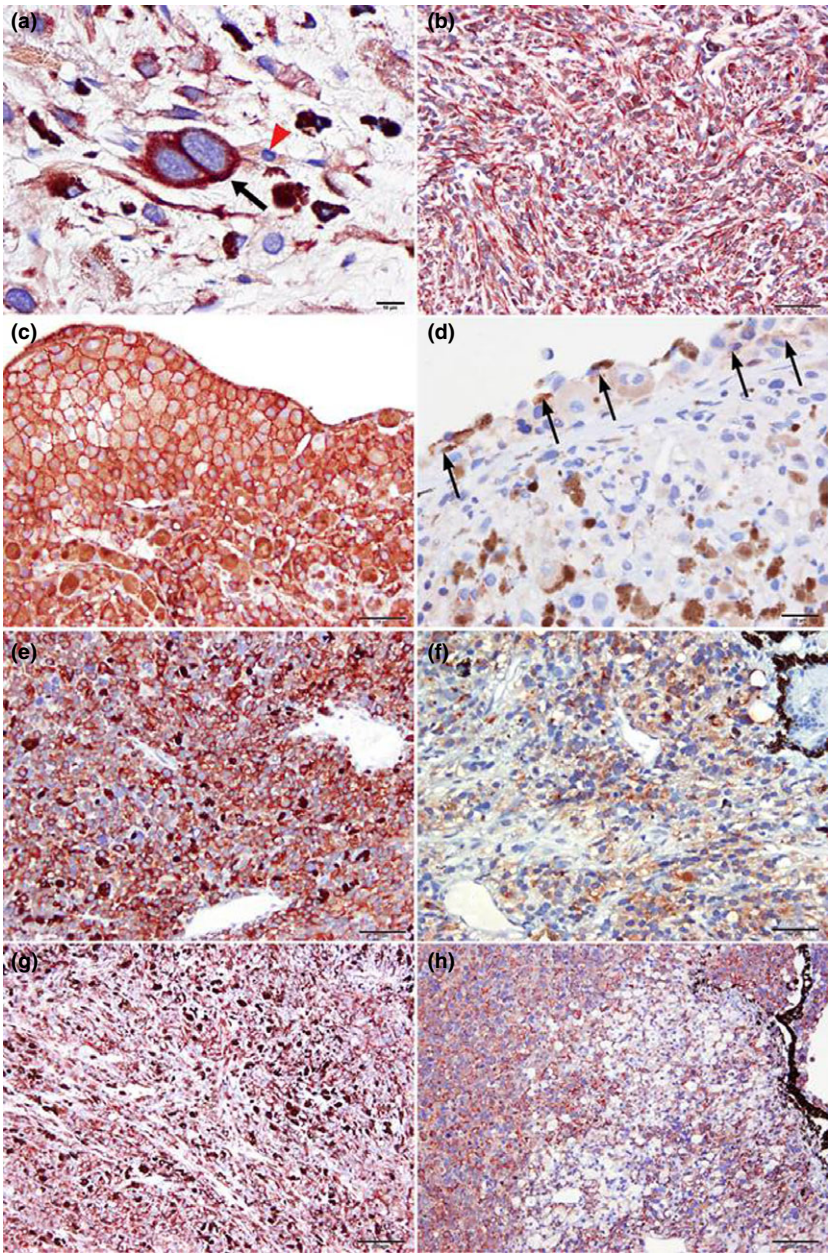

Figure 3. Immunohistochemical labeling of histologic sections of globes diagnosed with feline diffuse iris melanoma (FDIM). For all images, chromagen (indicating labeling) is orange-red, compared with the light- to dark-brown melanin. (a) B-Raf labeling of a FDIM with strong labeling of a neoplastic melanocyte (arrow) and less intense labeling of a morphologically normal melanocyte (arrowhead) (×600 magnification, bar = 10 μm). (b) Strong, homogenous B-Raf labeling of neoplastic melanocytes within a globe with FDIM (×200 magnification, bar = 40 μm). (c and d) E-cadherin labeling of neoplastic melanocytes within the iris stroma (c) and on the iris surface (d). Note the strong E-cadherin labeling of cell membranes of the majority of cells in c (×200 magnification, bar = 40 μm) compared to labeling of only a few surface neoplastic melanocytes (arrows) in d (×400 magnification). (e and f) Melan-A labeling of neoplastic cells (×200 magnification, bar = 40 μm). Note the homogenous strong red-brown cytoplasmic labeling of neoplastic cells in e compared to the mild melan-A labeling of neoplastic cells in f. (g and h) PNL2 labeling of neoplastic cells (×100 magnification, bar = 100 μm). Note the homogenous (g) or heterogeneous (h) labeling of neoplastic cells.

and their metastases did not.[34] This knowledge will facilitate exploration of therapeutic options. For example, melan-A is recognized by T lymphocytes.[35] Therefore, cats with FDIM expression of melan-A may be candidates for immunotherapy using vaccines or genetically modified cytotoxic T lymphocytes.

PNL2 is a monoclonal antibody directed against an unknown antigen associated with cells of melanocytic origin.[11] It is more sensitive and specific for the identification of human head and neck mucosal malignant melanomas than is melan-A or S100,[36] and more sensitive than melan-A and tyrosinase for the identification of canine melanocytic neoplasms, with a near 100% sensitivity when used in conjunction with melan-A.[37] To the authors' knowledge, however, PNL2 expression of feline melanocytic neoplasms has not been reported, and its utility as a prognostic indicator in melanocytic neoplasms in any species is unknown. Data from the present study reveal that PNL2 labeling intensity and homogeneity are reduced in metastatic FDIM suggesting that decreased expression of this melanocytic marker may indicate more aggressive biologic behavior. Because almost 70% of neoplastic cells labeled strongly with PNL2, prediction of metastasis in individual cats with FDIM may be more reliably achieved through analysis of label intensity of this immunohistochemical marker than of other immunohistochemical markers tested in the present study. Verification of these data and further exploration of this relationship in uveal melanocytic neoplasms of other species as well as melanocytic neoplasms from nonocular sites would be very valuable.

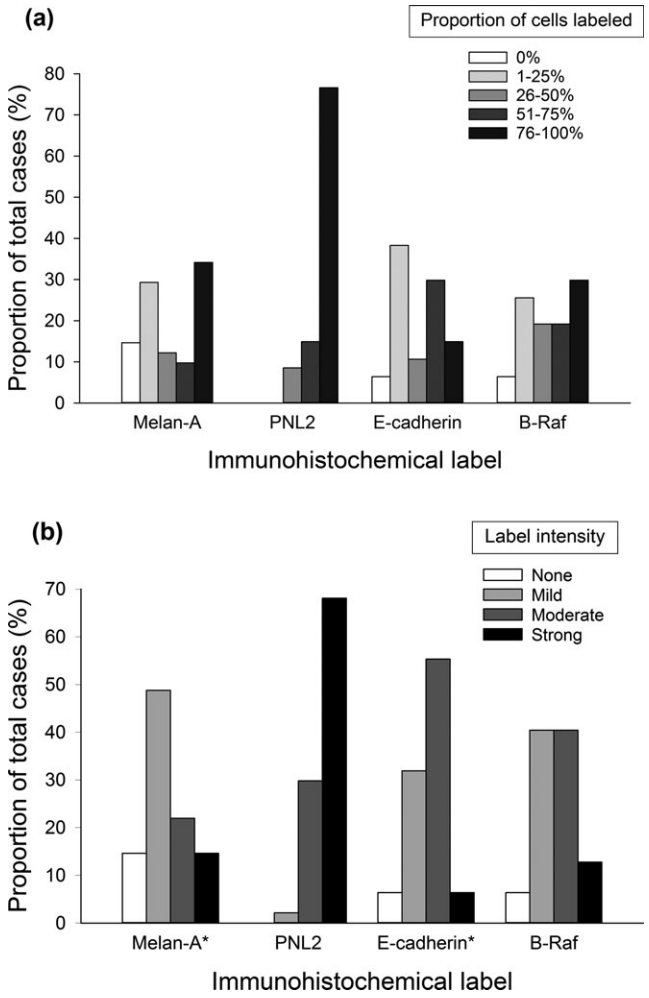

Figure 4. Percentage of neoplastic cells immunohistochemically labeled (a) and label intensity (b) for melan-A (41 globes with feline diffuse iris melanoma [FDIM]) or for PNL2, E-cadherin, or B-Raf (47 globes with FDIM). *Immunohistochemical stains for which increased label intensity was significantly associated with increased rate of metastasis.

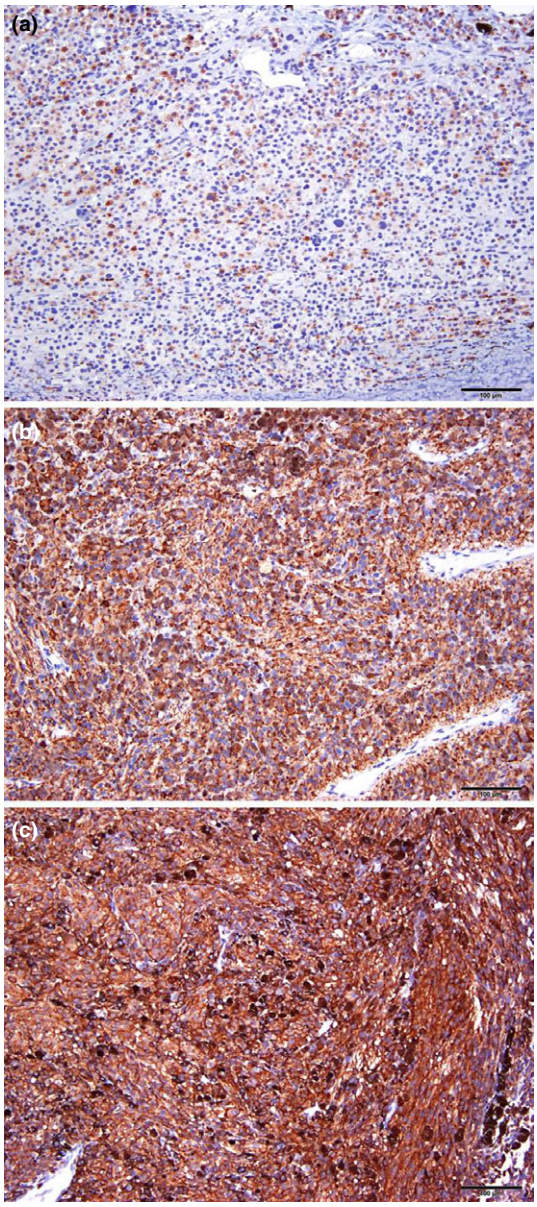

Figure 5. Representative images of immunolabeling intensity for PNL2 (a = mild, b = moderate, c = strong [×100 magnification, bar = 100 μm]).

E-cadherin, a transmembrane protein responsible for cell adhesion, plays an important role in metastasis of human cutaneous malignant melanomas.[12] Re-establishment of E-cadherin expression by melanocytic neoplastic cells *in vitro* prevents proliferation and migration, restores keratinocyte-mediated growth control,[38,39] and inhibits pulmonary metastasis in a murine model of malignant melanoma.[40] In human uveal malignant melanomas, however, neoplasms with increased risk of metastasis have epithelioid morphology and demonstrate upregulation of genes associated with this phenotype including E-cadherin.[41] Furthermore, upregulation of the E-cadherin gene is associated with metastatic uveal melanocytic neoplasms in dogs.[42] Thus, it was not surprising to find in the present study that increased E-cadherin label intensity in FDIM conferred a fivefold increased rate of metastasis. This suggests that molecular behavior of FDIM is similar to that of uveal melanocytic neoplasms in other species, but not cutaneous melanocytic neoplasms. Epithelioid cell morphology, however, was not found to be a risk factor in this study. Thus it appears that the tissue in which melanocytic neoplasms arise contributes to E-cadherin significance.[41] As cutaneous melanocytic neoplasms arise from epithelium, downregulation of cell adhesion molecules would be necessary for these cells to leave the tissue of origin. In contrast, uveal melanocytic neoplasms do not arise within epithelium and increased adhesion molecule expression may facilitate metastasis to distant organs.

Surprisingly, none of the immunohistochemical label parameters for B-Raf was associated with rate of metastasis

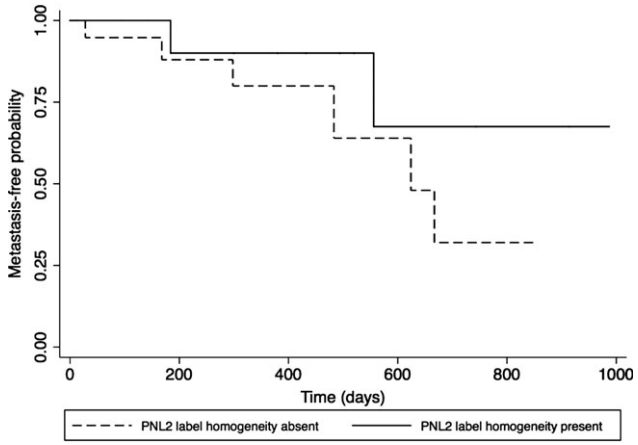

Figure 6. Kaplan–Meier plot showing the estimated probability of cats remaining metastasis-free as a function of time following enucleation and histologic diagnosis of FDIM with or without homogeneous PNL2 labeling.

in the present study. B-Raf is an oncoprotein with a role in the MAPK signaling pathway.[13–15] Gain-of-function B-Raf mutations lead to cellular proliferation and avoidance of apoptosis[14] and have been identified in cultured human uveal malignant melanoma cell lines and primary uveal malignant melanoma samples, but to a lesser extent compared to human cutaneous malignant melanomas.[17,18] Mice-possessing mutations in both the *BRAF* and *MC1R* genes have a higher rate of cutaneous malignant melanoma in the absence of UV-light stimulation than do darkly pigmented or albino mice.[43] The *MC1R* gene encodes the melanocortin 1 receptor, which is responsible for eumelanin production; inactivation of the receptor leads to a shift in melanin production to pheomelanin. Based on their histologic appearance, feline iridal melanocytes are believed to contain notable amounts of the lighter gold pheomelanin packaged in elongated melanosomes in addition to scattered dark brown to black eumelanin packaged in rounder melanosomes. Therefore, we hypothesized that B-Raf may be involved with the metastatic potential of FDIM. However, as we failed to show a significant association between B-Raf labeling and metastasis, B-Raf may only be a requirement for neoplasm development. Further studies are required to elucidate whether and in what manner the B-Raf we have identified in histologic samples of FDIM is mutated as this may prove to be an excellent molecular marker of metastasis as well as permit targeted therapies in future.[19–22]

A previous report identified a metastatic rate for FDIM of 63% and a mean survival time of only 156 days.[1] Another study published 3 years later reported a metastatic rate of 24%.[4] Compared with these reports, the metastatic rate and median survival time of cats in the present study were lower and higher, respectively. While direct comparisons between studies are difficult, this may represent an increasing awareness of the metastatic potential of FDIM. Unfortunately, high metastatic rates, in conjunction with a lack of reliable prognostic indicators, often lead clinicians to enucleate comfortable and visual globes in which FDIM is suspected in the hope that metastasis will be prevented. While histologic data provide some guidance for this decision, most require enucleated whole globes to make this decision. Future work should investigate whether histologic markers identified in the present study as significantly associated with metastasis are similarly useful when applied to incisional biopsy samples, iridal aspirates, or aqueocentesis samples containing free-floating neoplastic melanocytes as assessment of biopsy or cytologic specimens for these markers may help to prevent or delay enucleation. However, immunolabeling of cytologic samples would first require optimization and validation. The similarity between median times from diagnosis to detection of metastasis and to euthanasia because of suspected or confirmed metastasis in the present study highlights the importance of determining if adjunctive treatments such as chemotherapy or radiation therapy will prolong survival for those cats with enucleated globes demonstrating poor prognostic indicators. Additionally, regular staging of patients by use of thoracic radiographs and abdominal ultrasonography would also be required to determine if adjunctive treatments prolong the time between enucleation and detection of metastasis and between detection of metastasis and death. As no postoperative treatment protocols currently exist for FDIM, and no cats in this study received further treatment following surgery, future studies should examine the efficacy of adjunctive therapy in extending survival time by delaying metastasis. The median time of 20 days from initial presentation to enucleation indicates that most cats were not monitored for long prior to surgery. This study, however, did not determine exactly when iris color changes were first noted by the owner or primary care provider; as the majority of the globes were assessed by veterinary ophthalmologists following referral from general practitioners, the changes to the iris on ophthalmic examination were most likely advanced enough to warrant enucleation thus influencing the length of time between initial presentation and surgery.

In summary, the present study reveals that necrosis within the neoplasm, extrascleral extension of the neoplasm, a mitotic index of >7, and choroidal invasion each was significantly associated with a greater rate of metastasis in cats with FDIM. Furthermore, increased E-cadherin and melan-A label intensity were also associated with an increased rate of metastasis. Meanwhile, PNL2 is a marker of particular interest, with reduced labeling apparently associated with a poorer prognosis. While not associated with the development of metastasis in the present study, B-Raf remains a protein of interest given the presence of pheomelanin within the feline iris, and warrants investigation as a therapeutic target.

ACKNOWLEDGMENTS

The authors thank Mike Manzer for technical assistance with immunohistochemistry and John Doval for image preparation. This work was funded by the RM Cello Endowment, Vision for Animals Foundation resident research grant (grant number VAF2014-03), and Center for Companion Animal Health resident research fund (grant number 2013-39-R).

REFERENCES

1. Patnaik AK, Mooney S. Feline melanoma: a comparative study of ocular, oral, and dermal neoplasms. *Veterinary Pathology* 1988; **25**: 105–112.
2. Day MJ, Lucke VM. Melanocytic neoplasia in the cat. *Journal of Small Animal Practice* 1995; **36**: 207–213.
3. Dubielzig RR, Ketring KL, McLellan GJ *et al.* The uvea. In: *Veterinary Ocular Pathology: a Comparative Review*. 1st edn. Saunders Elsevier, New York, NY, 2010; 245–322.
4. Duncan DE, Peiffer RL. Morphology and prognostic indicators of anterior uveal melanoma in cats. *Progress in Veterinary and Comparative Ophthalmology* 1991; **1**: 25–32.
5. Kalishman JB, Chappell R, Flood LA *et al.* A matched observational study of survival in cats with enucleation due to diffuse iris melanoma. *Veterinary Ophthalmology* 1998; **1**: 25–29.
6. Planellas M, Pastor J, Torres MD *et al.* Unusual presentation of a metastatic uveal melanoma in a cat. *Veterinary Ophthalmology* 2010; **13**: 391–394.
7. Stiles J. Feline ophthalmology. In: *Veterinary Ophthalmology*, 5th edn. (eds Gellat KN, GIlger BC, Kern TJ) Wiley-Blackwell, Ames, IA, 2013; 1477–1559.
8. Koenig A, Wojcieszyn J, Weeks BR *et al.* Expression of S100a, vimentin, NSE, and melan A/MART-1 in seven canine melanoma cells lines and twenty-nine retrospective cases of canine melanoma. *Veterinary Pathology* 2001; **38**: 427–435.
9. Zhang Y, Jia R, Wang J *et al.* Targeted silencing of MART-1 gene expression by RNA interference enhances the migration ability of uveal melanoma cells. *International Journal of Molecular Sciences* 2013; **14**: 15092–15104.
10. Murer K, Urosevic M, Willers J *et al.* Expression of Melan-A/MART-1 in primary melanoma cell cultures has prognostic implication in metastatic melanoma patients. *Melanoma Research* 2004; **14**: 257–262.
11. Rochaix P, Lacroix-Triki M, Lamant L *et al.* PNL2, a new monoclonal antibody directed against a fixative-resistant melanocyte antigen. *Modern Pathology* 2003; **16**: 481–490.
12. McGary EC, Lev DC, Bar-Eli M. Cellular adhesion pathways and metastatic potential of human melanoma. *Cancer Biology Therapy* 2002; **1**: 459–465.
13. Davies H, Bignell GR, Cox C *et al.* Mutations of the BRAF gene in human cancer. *Nature* 2002; **417**: 949–954.
14. Gray-Schopfer V, Wellbrock C, Marais R. Melanoma biology and new targeted therapy. *Nature* 2007; **445**: 851–857.
15. Huang T, Karsy M, Zhuge J *et al.* B-Raf and the inhibitors: from bench to bedside. *Journal of Hematology and Oncology* 2013; **6**: 30–38.
16. Jang S, Atkins MB. Treatment of BRAF mutant melanoma: the role of vemurafenib and other therapies. *Clinical Pharmacology and Therapeutics* 2014; **95**: 24–31.
17. Henriquez F, Janssen C, Kemp EG *et al.* The T1799A BRAF mutation is present in iris melanoma. *Investigative Ophthalmology and Visual Science* 2007; **48**: 4897–4900.
18. Maat W, Kilic E, Luyten GP *et al.* Pyrophosphorolysis detects B-RAF mutations in primary uveal melanoma. *Investigative Ophthalmology and Visual Science* 2008; **49**: 23–27.
19. Mitsiades N, Chew SA, He B *et al.* Genotype-dependent sensitivity of uveal melanoma cell lines to inhibition of B-Raf, MEK, and Akt kinases: rationale for personalized therapy. *Investigative Ophthalmology and Visual Science* 2011; **52**: 7248–7255.
20. Bhatia S, Moon J, Margolin KA *et al.* Phase II trial of sorafenib in combination with carboplatin and paclitaxel in patients with metastatic uveal melanoma: SWOG S0512. *PLoS ONE* 2012; **7**: e48787.
21. Mahipal A, Tijani L, Chan K *et al.* A pilot study of sunitinib malate in patients with metastatic uveal melanoma. *Melanoma Research* 2012; **22**: 440–446.
22. Carvajal RD, Sosman JA, Quevedo JF *et al.* Effect of selumetinib vs chemotherapy on progression-free survival in uveal melanoma: a randomized clinical trial. *JAMA* 2014; **311**: 2397–2405.
23. Donaldson D, Sansom J, Scase T *et al.* Canine limbal melanoma: 30 cases (1992–2004). Part 1. Signalment, clinical and histological features and pedigree analysis. *Veterinary Ophthalmology* 2006; **9**: 115–119.
24. Spangler WL, Kass PH. The histologic and epidemiologic bases for prognostic considerations in canine melanocytic neoplasia. *Veterinary Pathology* 2006; **43**: 136–149.
25. Bujara K. Necrotic malignant melanomas of the choroid and ciliary body. A clinicopathological and statistical study. *Graefe's Archives for Clinical and Experimental Ophthalmology* 1982; **219**: 40–43.
26. Roels S, Tilmant K, Ducatelle R. PCNA and Ki67 proliferation markers as criteria for prediction of clinical behaviour of melanocytic tumours in cats and dogs. *Journal of Comparative Pathology* 1999; **121**: 13–24.
27. Laprie C, Abadie J, Amardeilh MF *et al.* MIB-1 immunoreactivity correlates with biologic behaviour in canine cutaneous melanoma. *Veterinary Dermatology* 2001; **12**: 139–147.
28. Millanta F, Fratini F, Corazza M *et al.* Proliferation activity in oral and cutaneous canine melanocytic tumours: correlation with histological parameters, location, and clinical behaviour. *Research in Veterinary Science* 2002; **73**: 45–51.
29. Bergin IL, Smedley RC, Esplin DG *et al.* Prognostic evaluation of Ki67 threshold value in canine oral melanoma. *Veterinary Pathology* 2011; **48**: 41–53.
30. Grahn BH, Peiffer RL, Cullen CL *et al.* Classification of feline intraocular neoplasms based on morphology, histochemical staining, and immunohistochemical labeling. *Veterinary Ophthalmology* 2006; **9**: 395–403.
31. Smith SH, Goldschmidt MH, McManus PM. A comparative review of melanocytic neoplasms. *Veterinary Pathology* 2002; **39**: 651–678.
32. Ramos-Vara JA, Miller MA, Johnson GC *et al.* Melan A and S100 protein immunohistochemistry in feline melanomas: 48 cases. *Veterinary Pathology* 2002; **39**: 127–132.
33. Kay PA, Pinheiro AD, Lohse CM *et al.* Desmoplastic melanoma of the head and neck: histopathologic and immunohistochemical study of 28 cases. *International Journal of Surgical Pathology* 2004; **12**: 17–24.
34. de Vries TJ, Trancikova D, Ruiter DJ *et al.* High expression of immunotherapy candidate proteins gp100, MART-1, tyrosinase and TRP-1 in uveal melanoma. *British Journal of Cancer* 1998; **78**: 1156–1161.
35. Kawakami Y, Eliyahu S, Delgado CH *et al.* Cloning of the gene coding for a shared human melanoma antigen recognized by

autologous T cells infiltrating into tumor. *Proceedings of the National Academy Sciences U S A* 1994; **91**: 3515–3519.
36. Morris LG, Wen YH, Nonaka D *et al.* PNL2 melanocytic marker in immunohistochemical evaluation of primary mucosal melanoma of the head and neck. *Head and Neck* 2008; **30**: 771–775.
37. Ramos-Vara JA, Miller MA. Immunohistochemical identification of canine melanocytic neoplasms with antibodies to melanocytic antigen PNL2 and tyrosinase: comparison with Melan A. *Veterinary Pathology* 2011; **48**: 443–450.
38. Hsu MY, Meier FE, Nesbit M *et al.* E-cadherin expression in melanoma cells restores keratinocyte-mediated growth control and down-regulates expression of invasion-related adhesion receptors. *American Journal of Pathology* 2000; **156**: 1515–1525.
39. Hirano T, Satow R, Kato A *et al.* Identification of novel small compounds that restore E-cadherin expression and inhibit tumor cell motility and invasiveness. *Biochemical Pharmacology* 2013; **86**: 1419–1429.
40. Lee DJ, Kang DH, Choi M *et al.* Peroxiredoxin-2 represses melanoma metastasis by increasing E-Cadherin/beta-Catenin complexes in adherens junctions. *Cancer Research* 2013; **73**: 4744–4757.
41. Onken MD, Ehlers JP, Worley LA *et al.* Functional gene expression analysis uncovers phenotypic switch in aggressive uveal melanomas. *Cancer Research* 2006; **66**: 4602–4609.
42. Malho P, Dunn K, Donaldson D *et al.* Investigation of prognostic indicators for human uveal melanoma as biomarkers of canine uveal melanoma metastasis. *Journal of Small Animal Practice* 2013; **54**: 584–593.
43. Mitra D, Luo X, Morgan A *et al.* An ultraviolet-radiation-independent pathway to melanoma carcinogenesis in the red hair/fair skin background. *Nature* 2012; **491**: 449–453.